Increasing the lateral resolution of 4Pi fluorescence microscopes

Nicolas Sandeau and Hugues Giovannini

Institut Fresnel, Unité Mixte de Recherche UMR 6133, Centre National de la Recherche Scientifique, Université Paul Cézanne–EGIM Nord, 13397 Marseille Cedex 20, France

Received March 11, 2005; revised August 30, 2005; accepted November 6, 2005; posted November 8, 2005 (Doc. ID 60755)

The axial resolution of fluorescence microscopes can be considerably improved by superposing two illumination beams and by adding coherently the two wavefronts emitted by the luminescent sample. This solution has been implemented in 4Pi microscopes. Theoretical and experimental results have shown that a considerable improvement of the axial resolution can be obtained with these microscopes. However, the lateral resolution remains limited by diffraction. We propose a configuration of a 4Pi microscope in which the lateral displacement of the source modifies the collection efficiency function (CEF). Numerical calculations based on an approximate scalar theory and on exact vector-wave-optics results of the field distribution of the electromagnetic field in image space show that the lateral extent of the CEF can be reduced by a factor greater than 2 with respect to the diffraction limit. We show that, with this solution, the resolution in the transverse plane of 4Pi type B and 4Pi type C microscopes can be improved significantly.

OCIS codes: 180.1790, 180.2520, 260.3160, 300.2530.

1. INTRODUCTION

Strong efforts have been made in the past decade to improve the resolution of fluorescence microscopes. Indeed, detecting the motion of luminophores inside cells or on cell membranes with subwavelength accuracy gives useful information for DNA and protein analyses, for the study of molecular dynamics, or for the study of single-biomolecule dynamics in fluid media. The volume of the point-spread function (PSF), which depends on the numerical aperture (NA) of the objective and on the wavelengths of the emission and of the excitation light, determines the resolution of fluorescence microscopes. In conventional confocal microscopes and for large-NA lenses, the resolution in the transverse direction is well approximated by $\lambda/2n$ where λ is the wavelength of light and n is the refractive index of the medium. This resolution is approximately four times better than the resolution obtained along the longitudinal direction ($2\lambda/n$). To reduce the axial length of the PSF, different arrangements with interference phenomena have been proposed.[1,2] The use of two opposite microscope objectives to coherently illuminate the fluorescent sample from both sides and to collect the fluorescence on both sides has led to the development of the so-called 4Pi microscope.[3] In this system the geometry of the PSF is determined by the pattern of the wavefronts interfering in the focal volume.[4] In practice, interference fringes whose visibility decreases when the distance between the fluorescent sample and the focus increases appear in the focal volume. The properties of this microscope have been extensively studied both theoretically[4–6] and experimentally,[7] and it has proved a resolution of 180 nm in the focal plane and 75 nm along the optical axis. In this paper we propose an arrangement based on the 4Pi microscope in which the lateral displacement of the luminophores modifies the spatial coherence of the two emitted wavefronts. The variations of the visibility of the interference fringes result in a reduction of the lateral extent of the collection efficiency function (CEF) of the microscope and therefore of the molecule-detection efficiency (MDE) function. In particular we show that, in certain cases, the lateral extent of the MDE can be two times smaller than the size determined by the diffraction limit.

Section 2 is dedicated to the description of the setup. In Section 3 we give a physical interpretation of the phenomena produced in the 4Pi′ microscope that led to an improvement of the lateral resolution. A scalar approach is used to calculate the CEF and the MDE in different cases. The influence of different parameters such as the NA of the objective, the magnification, and the size of the pinhole are discussed. In Section 4 the results obtained with a numerical simulation based on electromagnetic treatment of the problem are presented. Three-dimensional maps of the CEF and of the MDE are presented and quantitative results regarding the lateral resolution of the 4Pi′ microscope are given.

2. SETUP

Three major types of 4Pi microscopes have been reported.[5] In 4Pi type C microscopes the two incident wavefronts and the two emitted wavefronts are coherently added simultaneously. In 4Pi type A and 4Pi type B microscopes, the wavefronts are coherently added for illumination and for detection, respectively. In 4Pi-A microscopes, the resolution is determined by the excitation PSF, while in 4Pi-B and 4Pi-C microscopes the resolution is determined by the MDE with

$$\mathrm{MDE}(\mathbf{r}) = \mathrm{CEF}(\mathbf{r}) \cdot I_e(\mathbf{r}), \tag{1}$$

where $\mathbf{r}$ is the spatial vector that defines the position of the source; $\mathrm{CEF}(\mathbf{r})$ is the collection efficiency function al-

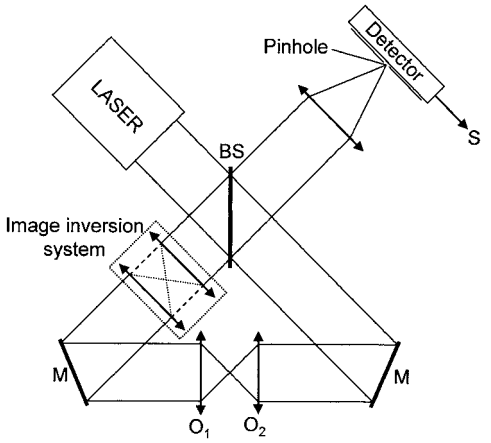

Fig. 1. Schematic of the 4Pi′ microscope. S, output signal; M, mirrors; BS, beam splitter; O_1 and O_2, microscope objectives. The optical paths in the two arms of the interferometer are assumed to be equal. The 4Pi′ arrangement is obtained from a 4Pi microscope[12] by adding an image inversion system in one arm of the interferometer.

ready defined, following Koppel *et al.*,[8] as the fraction of light emitted by a point source located at $\mathbf{r}$ that is focused on a detector; and $I_c(\mathbf{r})$ is the excitation field's intensity at $\mathbf{r}$. Several solutions have been proposed to modify the PSF or the MDE of 4Pi microscopes. It has been shown that the height of the sidelobes of the MDE of 4Pi-C microscopes along the optical axis can be reduced by adding in the illumination path multiring phase-only pupil filters.[9–11] However, these solutions do not lead to an improvement of the lateral resolution. To improve this lateral resolution we propose a configuration of the 4Pi microscope in which the spatial coherence of the two emitted beams depends on the displacement of the luminophore in a plane perpendicular to the optical axis. In this case, the spatial distribution of the intensity on the photodetector resulting from the coherent superposition of the two emitted beams depends on the distance d between the luminophore and the optical axis. This system, which we call the 4Pi′ microscope, is a 4Pi microscope in which an image inversion system has been added in one arm of the interferometer (see Fig. 1). The image inversion system modifies the symmetry of the optical conjugations in a manner that will be discussed in Section 3. We assume that the optical path difference between the two arms of the interferometer is equal to zero with a perfectly compensated chromatic dispersion. To predict the properties of the 4Pi′ microscope, we give (in Section 3) a physical interpretation of the phenomena produced by the particular geometry of the system.

3. PHYSICAL INTERPRETATION

The rules of geometrical optics show that the 4Pi′ microscope is equivalent to a system in which two beams are emitted by two coherent sources that are symmetric with respect to focus. In Fig. 2 we have represented the scheme of the sensor head equivalent to a 4Pi microscope and to a 4Pi′ microscope. In this figure we considered a dipole source to show the symmetries obtained with the two arrangements. From Fig. 2 one can see that, in a standard 4Pi microscope, the two sources are symmetric with respect to the focal plane. In the 4Pi′ microscope, when the dipole moves in a direction perpendicular to the optical axis, the presence of the image inversion system modifies the symmetry of the optical conjugations. In this case the 4Pi′ microscope is equivalent to a system in which two beams are emitted by two sources symmetric with respect to the focus F of the microscope objective. The two emitted beams are coherently added on the detector. The output signal is proportional to the mean field's intensity on the photodetector. When the distance between the luminophore and the optical axis increases, the visibility of the interference signal recorded by the detector decreases. Thus one can expect a CEF with a 4Pi′ microscope different from the CEF obtained with a 4Pi microscope. To study the modifications of the CEF caused by the presence of the image inversion system in one arm of the interferometer, we have used a simplified approach. We have considered a point source S located in the common focal plane of the microscope objectives and we have used a scalar theory of diffraction. The spherical wave emitted by the source is collected on each side by the microscope objectives and the two collimated beams are sent to the detector. The optical conjugations described by Fig. 3 show that the 4Pi′ microscope is equivalent to a system in which the beams emitted by two point sources S and IS that are symmetric with respect to focus F are superimposed on the detector. The intensities of the beams emitted by S and IS are assumed to be equal. In this case the intensity in the focal plane F_L of lens L for the 4Pi microscope is given by

$$I_d(x,y) = \left[\frac{J_1(u^-)}{u^-}\right]^2, \tag{2}$$

$$I_d(x,y) = \left[\frac{J_1(u^+)}{u^+} + \frac{J_1(u^-)}{u^-}\right]^2 \tag{3}$$

for the 4Pi′ microscope, with

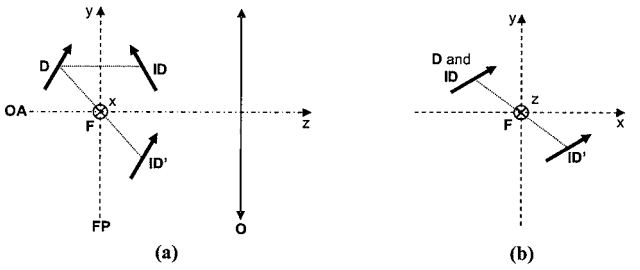

Fig. 2. Schematic representation of the sensor head of a system equivalent to a 4Pi microscope and of a system equivalent to a 4Pi′ microscope. F is the common focus of the two microscope objectives O_1 and O_2. O is a microscope objective identical to O_1 or to O_2 (O_1 and O_2 are assumed to be identical). OA is the optical axis of the system. Dipole D is the dipole emitter. D moves in the vicinity of the focal plane FP. ID is the image of D through the 4Pi microscope. ID' is the image of D through a 4Pi′ microscope. In this representation, the beams emitted by D and by ID for the 4Pi microscope and by D and by ID' for the 4Pi′ microscope pass through O and are superimposed on the detector. (a) View in a plane containing the optical axis. (b) View in a plane orthogonal to the optical axis.

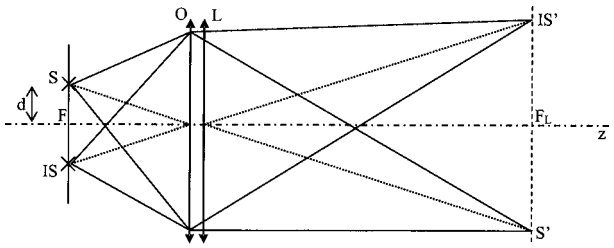

Fig. 3. Optical system equivalent to a 4Pi′ microscope. O is the microscope objective (the two microscope objectives O_1 and O_2 are assumed to be identical). S is the source that moves in the focal plane of O. S emits a spherical wave. A second spherical wave is emitted by IS. S and IS are symmetrical with respect to F. S' and IS' are the images, through the optical system $(O;L)$, of S and IS', respectively.

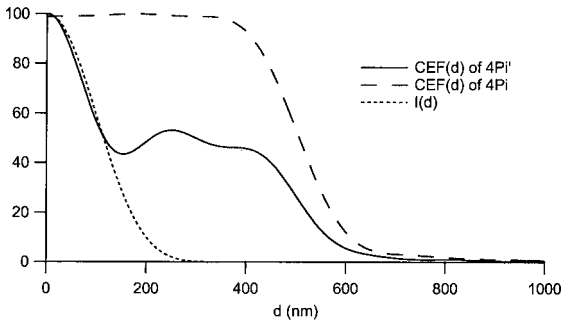

Fig. 4. Section of the CEF of the 4Pi and the 4Pi′ microscopes in arbitrary units in the focal plane of the microscope objective. The source emits at $\lambda=525$ nm. The diameter of the detector is $\phi=100$ μm. $M=100$ and NA=1.45. The intensity I of the pump beam at 488 nm, focused by O, is also represented.

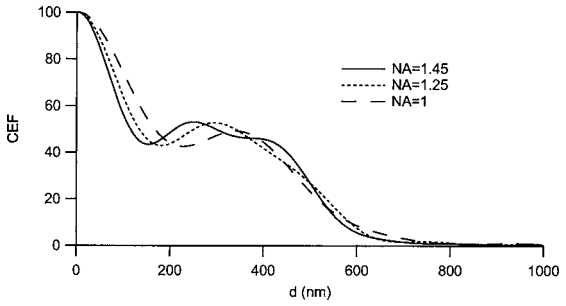

Fig. 5. Sections of the CEF of the 4Pi′ microscope obtained with different microscope objectives. $\lambda=525$ nm. NA=1.45, with $m=100$ corresponding to an α Plan-FLUAR objective from Zeiss. NA=1.25 and NA=1, with $m=100$ corresponding to an N Plan-FLUAR microscope objective NA=1.25–0.6×100 from Leica.

$$u^{-}=\frac{k\mathrm{NA}}{m}\sqrt{(x-md)^2+y^2}, \tag{4}$$

$$u^{+}=\frac{k\mathrm{NA}}{m}\sqrt{(x+md)^2+y^2}, \tag{5}$$

where ϕ is the diameter of the microscope objective, d is the distance between S and F, m is the magnification of the optical system composed of O and L, NA is the numerical aperture of O, and $k=2\pi/\lambda$ where λ is the wavelength of the light emitted by S. For each value of distance d, the signal delivered by the photodetector centered on F_L is proportional to the signal (Sig) given by

$$\mathrm{Sig}(d)=\int_{S_{\mathrm{PD}}}\int I_d(x,y)\mathrm{d}x\mathrm{d}y, \tag{6}$$

where S_{PD} is the surface of the photodetector. The section of the CEF in the focal plane of O is obtained by varying d.

To study the influence of the characteristics of O and L, we have computed Sig(d) using Eq. (6). A comparison between the CEF of the 4Pi and the 4Pi′ microscopes is shown in Fig. 4. We have considered the case of luminophores emitting at $\lambda=525$ nm, which is a typical value for luminescent markers commonly used for biology applications. For the 4Pi microscope, when the values of NA, m, and the diameter ϕ of the detector are such that the size of the figures of diffraction centered on S' and IS' is smaller than ϕ, the full width at half-maximum (FWHM) of the CEF is determined by ϕ. For the 4Pi′ microscope, the CEF exhibits a peak that is obtained when S is the vicinity of F. When S is located on F, the two figures of diffraction, centered on S' and IS', are superimposed and the CEF reaches its maximum value. The width of this peak depends only on m and NA. When d increases, S' and IS' move symmetrically with respect to F_L, and the CEF, which is the result of an average of the intensity on the detector, decreases. When S' and IS' are outside of the detector, the CEF tends to zero. Figure 5 shows the CEF of the 4Pi′ microscope calculated for different values of NA. One can see that, for a given value of m, the FWHM of the central peak decreases when NA increases. Indeed, when NA increases, the size of the figures of diffraction centered on S' and IS' (see Fig. 3) decreases and the effect of the averaging produced by the detector becomes significant for smaller values of d.

For most applications fluorescence microscopy is made with luminophores pumped by an incident beam. In these cases the resolution is given by the MDE function given by Eq. (1). The MDE is the product of the CEF by the incident intensity. In Fig. 4 we have represented the intensity distribution, in the focal plane of O, of the pump beam. We have considered a monochromatic incident argon beam at $\lambda=488$ nm that can be used to pump the fluorescence of luminophores emitting around 525 nm. In Fig. 5 we have represented the MDE, which is calculated using Eq. (1), obtained with 4Pi and 4Pi′ microscopes in the case of a high-numerical aperture (NA=1.45) microscope objective. One can see that a significant improvement is obtained with the 4Pi′ arrangement. To give quantitative results concerning the resolution of the 4Pi′ microscope, we have used a numerical simulation based on the electromagnetic theory of diffraction.

4. ELECTROMAGNETIC TREATMENT

To test the validity of the results presented in Section 3, and to study the three-dimensional properties of the CEF and the MDE, we have made numerical calculations by using the approach developed by Richards and Wolf[13] and later applied to the calculation of the CEF by Enderlein.[14,15] The source considered is a dipole emitter.

We have computed the CEF and the MDE of the optical systems equivalent to the 4Pi and the 4Pi′ microscopes (see Fig. 2). The dipole emitter was considered to be immersed in an homogeneous medium and no cover glass was considered.[16–18] As the FWHM of the typical emission spectrum of the most common luminophores used in fluorescence correlation spectroscopy experiments is ~20 nm, the CEF of the 4Pi′ microscope has been calculated by assuming a monochromatic emission. The CEF was averaged for each position of the dipole emitter over all possible dipole orientations, corresponding to imaging fluorescing molecules with a rotation diffusion much faster than the fluorescence lifetime. The averaged CEF was calculated for different positions of the dipole emitter around focus F. A comparison between the CEF of a 4Pi microscope and the CEF of a 4Pi′ microscope is shown in Fig. 6. One can see from Fig. 6(b) the particular shape of the CEF of the 4Pi′ microscope due to the symmetry described in Fig. 2. In Fig. 6(c) one can see the effect of the displacement of the dipole in the focal plane. These results confirm the preliminary conclusions of Section 3. When the dipole is located on focus F, the amplitude of the signal recorded by the detector reaches its maximum value. This amplitude decreases when the dipole moves along the x or y axis and gradually, as d increases, signal S tends to reach a mean value that is the continuous background. For higher values of d, the two beams do not pass through the pinhole anymore and the CEF tends to zero. The calculations have been made by considering a pinhole whose diameter is equal to 20 μm (which is a size commonly used in fluorescence microscopy experiments), two oil immersion microscope objectives with NA=1.4, and a magnification $m=40$. These characteristics are typical of 4Pi microscopes. One can see that, in this case, the

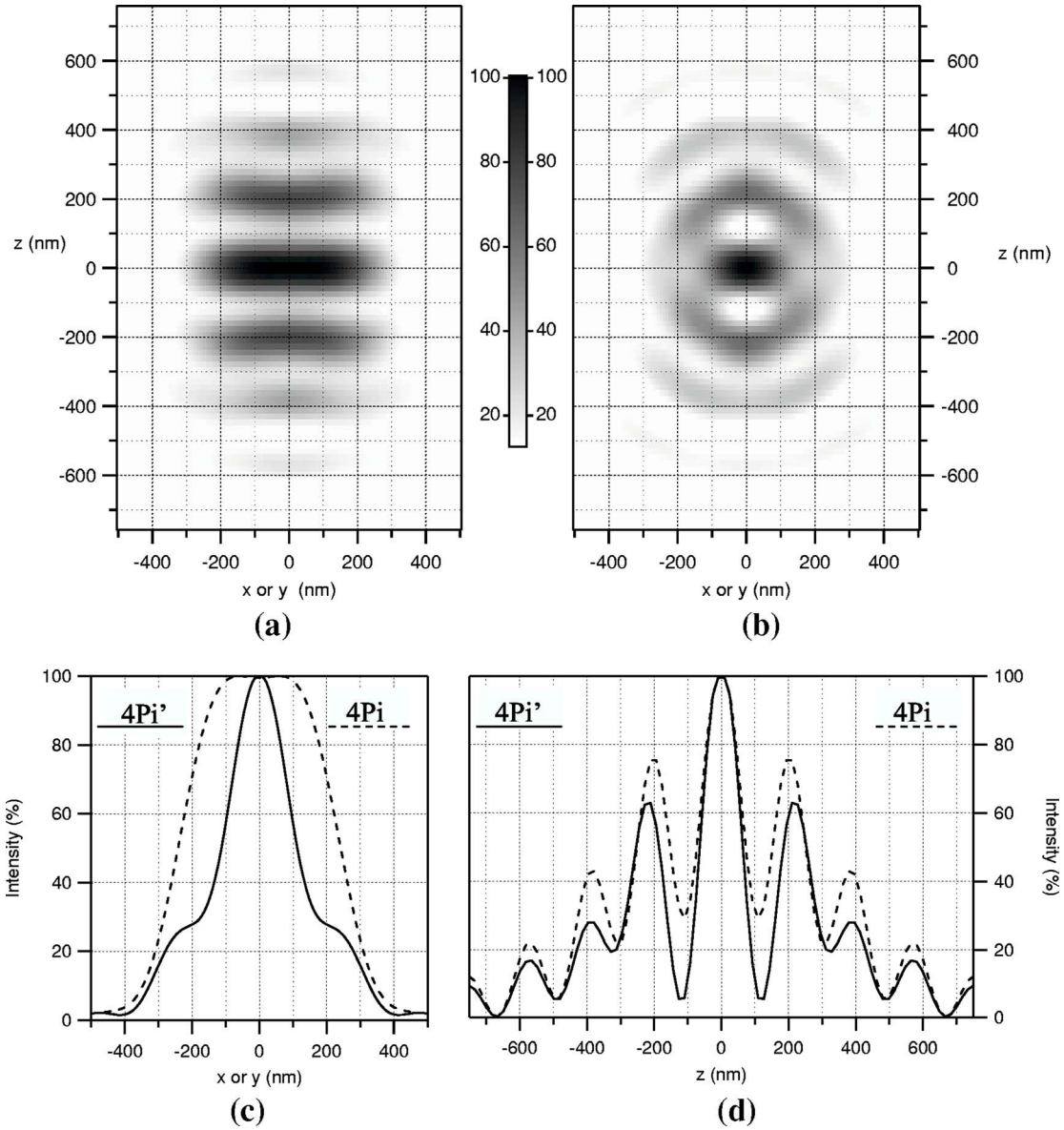

Fig. 6. (a), (b) Comparison between the calculated CEF (arbitrary units) of (a) a 4Pi microscope and (b) a 4Pi′ microscope. (c) Section of the CEF in the transverse plane. (d) Section of the CEF along the optical axis. The diameter ϕ of the pinhole is $\phi=20$ μm. The wavelength of emission is $\lambda_2=525$ nm. In the numerical calculation, the microscope objectives O_1 and O_2 are oil immersion objectives (NA =1.4, magnification $m=40$).

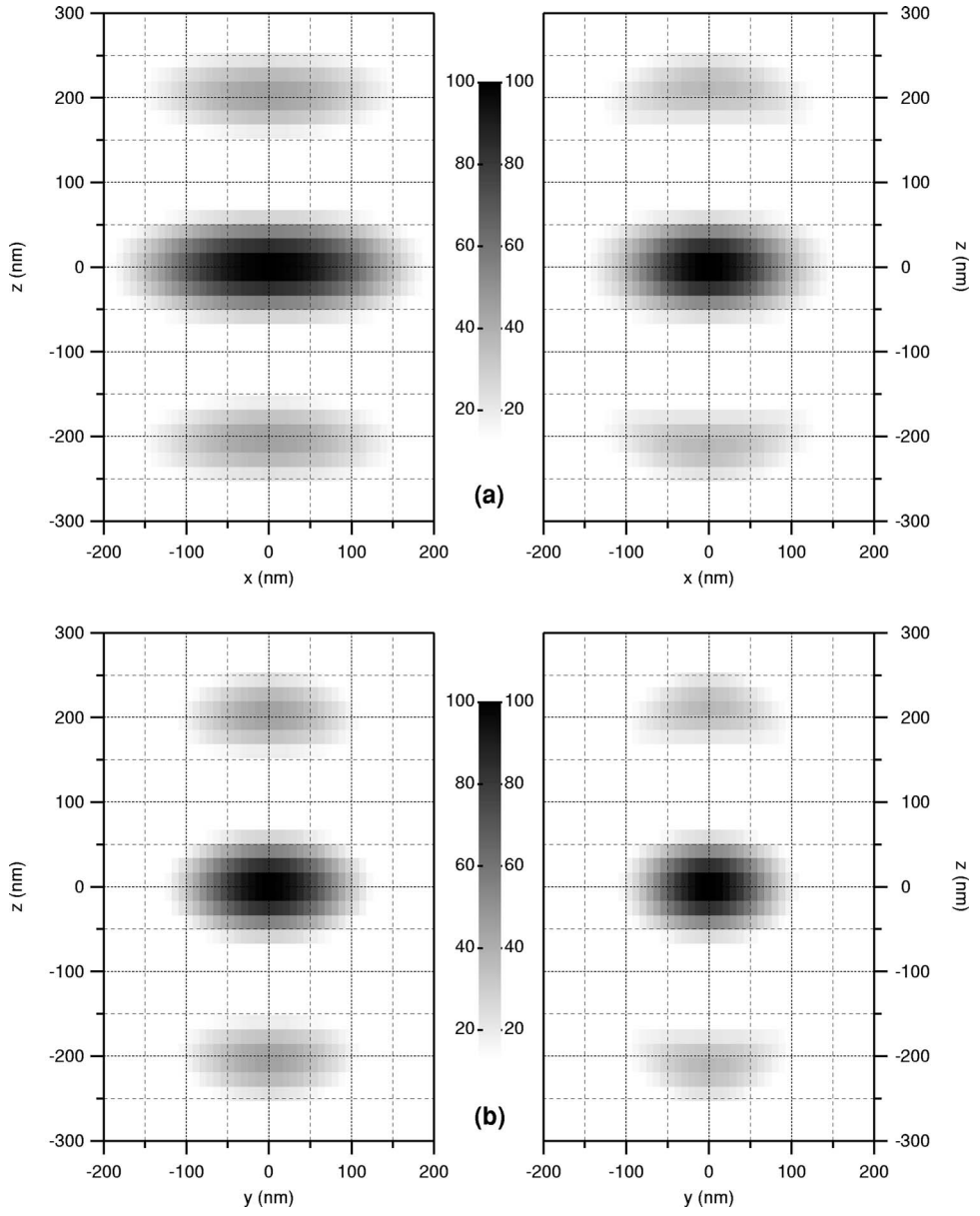

Fig. 7. Comparison between the calculated MDE (arbitrary units) of a 4Pi microscope and the calculated MDE of a 4Pi′ microscope. The illumination beam is a Gaussian monochromatic beam (emission wavelength $\lambda_1=488$ nm) linearly polarized along the x axis. (a) MDE of the 4Pi-C microscope (left) and MDE of a 4Pi′-C microscope (right) in the $x-y$ plane. (b) MDE of the 4Pi-C microscope (left) and MDE of a 4Pi′-C microscope (right) in the $y-z$ plane.

FWHM of the CEF is reduced by a factor of 2.14 with respect to a standard 4Pi microscope. The lateral resolution is 113 nm at wavelength $\lambda_2=525$ nm, that is, a resolution of $\lambda/4.65$ with a microscope objective with NA=1.4. This result shows that a strong improvement is obtained with respect to the 4Pi microscope. On the other hand, along the optical axis, the section of the CEF of the 4Pi′ microscope is almost similar to that of a 4Pi microscope. However, the symmetry of the dipoles shown in Fig. 2 leads to an attenuation of the sidelobes. These results suggest that the 4Pi′ microscope can locate any emitter (electroluminescent, bioluminescent, etc.) in the transverse direction with a much better resolution than a conventional 4Pi microscope.

For a photoexcitation experiment, the incident field has to be considered and the resolution is determined by the MDE of the microscope. We assume that the two incident pump beams are added coherently. In this case the microscope is either a 4Pi′ type C or a 4Pi′ type C microscope, depending on whether the image inversion system is placed in one arm of the interferometer. We assume that the optical path difference between the two incident beams is equal to zero on focus F and we neglect the effects of chromatic dispersion. The excitation field's intensity $I_e(\mathbf{r})$ was calculated for the 4Pi-C and 4Pi′-C microscopes by considering incident linearly polarized Gaussian beams. The MDE was calculated by Using Eq. (1). As an inversion system is placed in one arm of the 4Pi′-C microscope, to preserve the spatial coherence of the two incident wavefronts, the laser needs to be transverse monomode. For this reason, we assume that the pump beams are emitted by the same monomode TEM_{00}

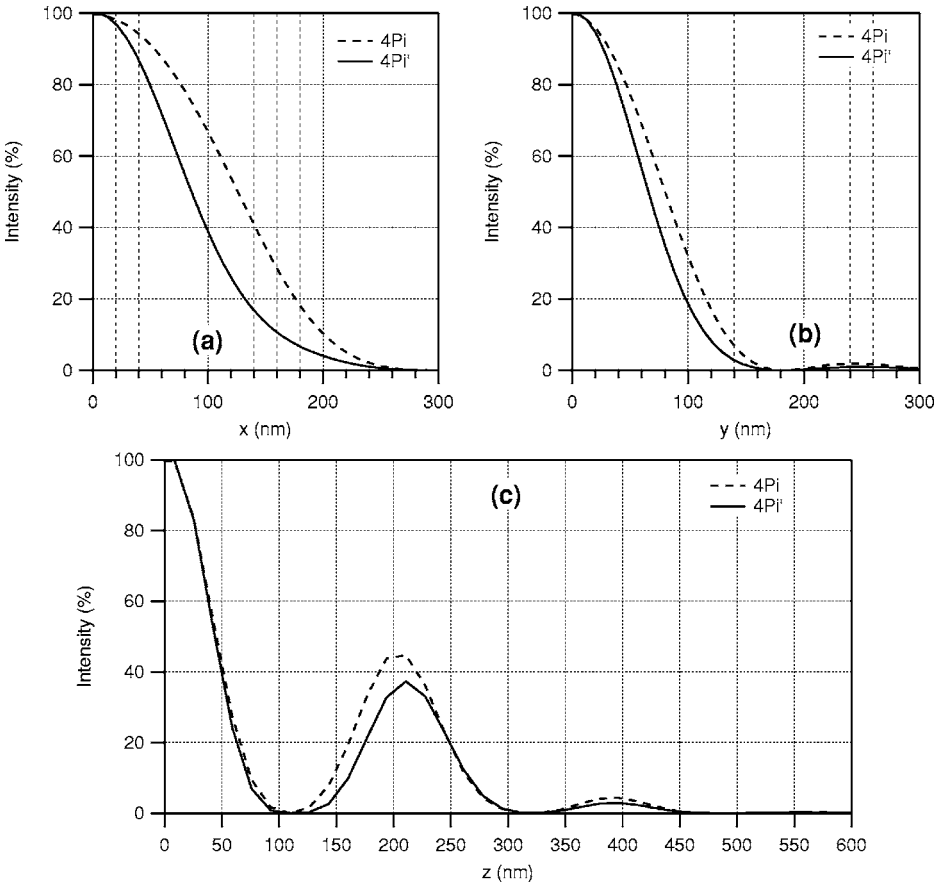

Fig. 8. Comparison between the MDE (arbitrary units) of a 4Pi-C microscope and the MDE of a 4Pi′-C microscope. (a) Section of the MDE in the focal plane along the x axis. (b) Section of the MDE in the focal plane along the y axis. (c) Section of the MDE along the z axis.

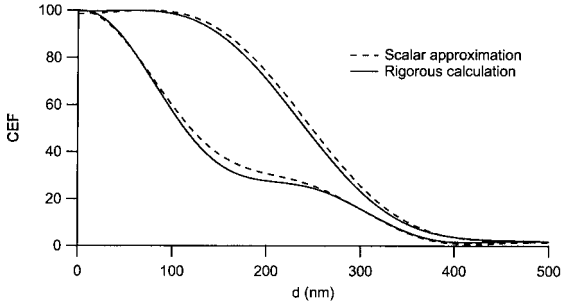

Fig. 9. CEF (arbitrary units) calculated with two different methods. In both calculations, $\lambda=525$ nm, NA=1.4, $m=40$, $\phi=20$ μm.

laser. Figure 7 shows the MDE calculated for 4Pi-C and 4Pi′-C microscopes. From Fig. 8, one can see that, depending on the direction of polarization of the incident beams and on the size of the detector, one can obtain, with a 4Pi′-C microscope, a reduction of the lateral extent of the MDE varying between 19.3% and 29.5% with respect to a classical 4Pi microscope. Figure 8(c) shows that, as for the CEF, the sidelobes of the MDE of the 4Pi′ microscope are attenuated with respect to those of the 4Pi microscope.

To determine whether a rigorous approach is essential for evaluating the CEF or the MDE of a 4Pi′ microscope in the focal plane of the microscope objective, we have compared the CEF calculated with the scalar-approximated method described in Section 3 to the averaged CEF calculated with the theory used in Section 4. A comparison between the results is shown in Fig. 9. One can see that the approach developed in Section 3, which gives a good approximation of the CEF, can be used to determine the influence of the parameters $(\mathrm{NA}, m, \phi, \lambda)$ of the system.

5. CONCLUSION

We have shown that, by adding an inversion system in one arm of the 4Pi microscope (for the typical values of the numerical aperture, of the magnification of the microscope objective, and of the diameter of the pinhole used in fluorescence microscopes), the lateral extension of the CEF can be reduced by a factor greater than 2 with respect to the resolution determined by the diffraction limit. This result, which is obtained by taking advantage of the modification of the spatial coherence of the two emitted wavefronts produced by the displacement of the source around the focal plane of the microscope objectives, suggests that the 4Pi′ microscope can locate any emitter (electroluminescent, bioluminescent, etc.) in the transverse direction with a resolution better than that of a conventional 4Pi microscope. For a photoexcitation experiment, the improvement of the transverse resolution can be up to 29% with respect to a conventional 4Pi type C microscope. Various configurations using cylindrical lenses or reflecting corner cubes can be implemented to compen-

sate the chromatic dispersions of the two arms of the interferometer or to modify the symmetries of the optical conjugations resulting in a modification of the CEF. Moreover, the solution proposed in this paper is compatible with the use of stimulated emission depletion.[19]

The authors' e-mail addresses are nicolas.sandeau@fresnel.fr and hugues.giovannini @fresnel.fr.

REFERENCES

1. M. Nagorni and S. W. Hell, "Coherent use of opposing lenses for axial resolution increase in fluorescence microscopy. I. Comparative study of concepts," J. Opt. Soc. Am. A **18**, 36–48 (2001).
2. P.-F. Lenne, E. Etienne, and H. Rigneault, "Subwavelength patterns and high detection efficiency in fluorescence correlation spectroscopy using photonic structures," Appl. Phys. Lett. **80**, 4106–4108 (2002).
3. S. Hell, "Double-confocal scanning microscope," European patent application EP0491289 (June 24, 1992).
4. C. J. R. Sheppard and Y. Gong, "Improvement in axial resolution by interference confocal microscopy," Optik (Stuttgart) **87**, 129–132 (1991).
5. S. Hell and E. H. K. Stelzer, "Properties of a 4Pi confocal fluorescence microscope," J. Opt. Soc. Am. A **9**, 2159–2166 (1992).
6. M. Gu and C. J. R. Sheppard, "Three-dimensional transfer functions in 4Pi confocal microscopes," J. Opt. Soc. Am. A **11**, 1619–1627 (1994).
7. S. W. Hell, S. Lindek, C. Cremer, and E. H. K. Stelzer, "Measurement of the 4Pi-confocal point-spread function proves 75 nm axial resolution," Appl. Phys. Lett. **64**, 1335–1337 (1994).
8. D. E. Koppel, D. Axelrod, J. Schlessinger, E. L. Elson, and W. W. Webb, "Dynamics of fluorescence marker concentration as a probe of mobility," Biophys. J. **16**, 1315–1329 (1976).
9. C. M. Blanca, J. Bewersdorf, and S. W. Hell, "Single sharp spot in fluorescence microscopy of two opposing lenses," Appl. Phys. Lett. **79**, 2321–2323 (2001).
10. M. Martinez-Corraz, A. Pons, and M. T. Caballero, "Axial apodization in 4Pi-confocal microscopy by annular binary filters," J. Opt. Soc. Am. A **19**, 1532–1536 (2002).
11. M. Martinez-Corraz, M. T. Caballero, A. Pons, and P. Andrés, "Sidelobe decline in single-photon 4Pi microscopy by Toraldo rings," Micron **34**, 319–325 (2003).
12. H. Gugel, J. Bewersdorf, S. Jakobs, J. Engelhardt, R. Storz, and S. W. Hell, "Cooperative 4Pi excitation and detection yields sevenfold sharper optical sections in live-cell microscopy," Biophys. J. **87**, 4146–4152 (2004).
13. B. Richards and E. Wolf, "Electromagnetic diffraction in optical systems. II. Structure of the image field in an aplanatic system," Proc. R. Soc. London Ser. A **235**, 358–379 (1959).
14. J. Enderlein, "Theoretical study of detection of a dipole emitter through an objective with high numerical aperture," Opt. Lett. **25**, 634–636 (2000).
15. M. Bohmer and J. Enderlein, "Orientation imaging of single molecules by wide-field epifluorescence microscopy," J. Opt. Soc. Am. B **20**, 554–559 (2003).
16. S. H. Wiersma, P. Török, T. D. Visser, and P. Varga, "Comparison of different theories for focusing through a plane interface," J. Opt. Soc. Am. A **14**, 1482–1490 (1997).
17. P. Torok, "Propagation of electromagnetic dipole waves through dielectric interfaces," Opt. Lett. **25**, 1463–1465 (2000).
18. O. Haeberlé, "Focusing of light through a stratified medium: a practical approach for computing microscope point spread functions. Part I: Conventional microscopy," Opt. Commun. **216**, 55–63 (2003).
19. M. Dyba and S. W. Hell, "Focal spots of size lambda/23 open up far-field fluorescence microscopy at 33 nm axial resolution," Phys. Rev. Lett. **88**, 163901 (2002).